Available online at www.sciencedirect.com
ScienceDirect
Polymer 48 (2007) 1020–1029
polymer
www.elsevier.com/locate/polymer

Conductivity spectroscopy on melt processed polypropylene–multiwalled carbon nanotube composites: Recovery after shear and crystallization

Ingo Alig [a,*], Dirk Lellinger [a], Sergej M. Dudkin [a], Petra Pötschke [b]

[a] Deutsches Kunststoff-Institut (DKI), Schlossgartenstrasse 6, D-64289 Darmstadt, Germany
[b] Leibniz-Institut für Polymerforschung Dresden e.V. (IPF), Hohe Str. 6, D-01069 Dresden, Germany

Received 6 October 2006; accepted 19 December 2006
Available online 22 December 2006

Abstract

Frequency dependent investigations of conductivity and dielectric permittivity have been performed on composites of polypropylene (PP) containing different amounts of 2, 3.5, and 5 wt% of multiwalled carbon nanotubes (MWNTs) in the melt and during crystallization. The experiments were performed in a measurement slit die containing two dielectric sensors in plate–plate geometry, which was flanged to the outlet of a single screw laboratory extruder. AC conductivity and the related complex permittivity were measured in the frequency range from 20 Hz to 10^6 Hz after stopping the extruder (recovery after shearing) and during cooling (non-isothermal crystallization). For a sample with a MWNT content of 2 wt% the AC conductivity shows a tremendous increase with time after shearing was stopped. This conductivity recovery is explained by the reorganization of the conducting network-like filler structure, which was partially destroyed by the shear. The reformation kinetics of filler clusters is assumed to be due to a cooperative aggregation. For conductive fillers in a thermoplastic matrix the kinetics of cooperative aggregation is coupled to the electrical percolation. The reorganization of the percolation network can be related to reformation of (i) the local contact regions between the nanotubes (separated by polymer chains) and (ii) to the reorientation of nanotubes oriented in the shear flow. The conductivity recovery is less pronounced for samples with MWNT concentrations well above the percolation threshold. During cooling of the melt to temperatures below crystallization a significant decrease in the conductivity and permittivity was detected. This is consistently expressed in the conductivity and permittivity spectra and can be explained by reduction of the amorphous phase (high ion mobility) on expense of the crystalline phase and/or by crystalline regions in the contact region between tubes.

Keywords: Multiwalled carbon nanotube; Polymer composites; Electrical conductivity

1. Introduction

During the last years polymer composites based on carbon nanotubes (CNTs) have attracted much interest in developing new materials. In many investigations the property enhancement potential was studied by looking at electrical, mechanical, thermal and other properties (see reviews in Refs. [1–3]). It was found that due to the fibrous shape of the conductive filler electrical percolation in polymer based composites can occur at extremely low CNT contents, as low as 0.0025 wt% for MWNT in epoxy [4], 0.15–0.1 wt% for MWNT in polyimide prepared by in situ polymerization [5], or 0.05 vol% for MWNT melt mixed into polypropylene [6].

It was also found that the mechanical properties can be enhanced by adding low CNT amounts, especially modulus and strength but also toughness [7–9]. In addition, also other properties like thermal stability, fire behavior, wear behavior and others can be influenced favourably by using CNT as additives [10–12]. Whereas in earlier studies mainly solution based preparation and in situ polymerization of polymers in the presence of nanotubes were used, now also melt mixing of nanotubes into polymeric matrices plays an increasing role [2,6,13–15]. This method can be regarded to be the preferred method for industrial application of carbon nanotube–polymer

* Corresponding author. Tel.: +49 6151 16 2404; fax: +49 6151 29 2855.
E-mail address: ialig@dki.tu-darmstadt.de (I. Alig).

0032-3861/$ - see front matter © 2007 Elsevier Ltd. All rights reserved.
doi:10.1016/j.polymer.2006.12.035

composites for bulky materials. The issue of dispersion of synthesized nanotube agglomerates, and in case of single walled carbon nanotubes (SWNT) of SWNT bundles, is crucial for exploiting the extraordinary electrical and mechanical properties of CNT in composites. In industrial applications, dispersion is usually performed in extruders and it is of interest which state of dispersion can be reached during the shear and elongation stresses acting during melt processing.

Recently, our group reported on investigations with dielectric (conductivity) spectroscopy on solid polycarbonate–multiwalled carbon nanotube (MWNT) composites prepared by melt mixing for characterization of content and the state of nanotube dispersion [16]. This study demonstrates the sensitivity of conductivity spectroscopy for the investigation of polymer composites containing CNT and provides a strong indication that the nanotubes are separated at their contacts by polymer chains. These local contact regions can create considerable contact resistance and contact capacitance. More recently, our group reported on a combined melt rheological and dielectric investigation [17] of the influence of the polymer chains in this contact region between CNT on the mechanical and electrical properties. From both dielectric and rheological measurements, it was concluded that the percolation network formed by CNT in a polymer matrix has to be considered as a combined network built by nanotubes which are separated by local contact regions with polymer chains in-between. Therefore, the mechanical deformation during melt processing (here: extrusion) is expected to have a strong influence on the (conducting) filler network. This behavior is known from carbon black filled polymer composites. Since the reformation of the filler network (recovery of conductivity) takes considerably longer than the usual processing time (several minutes) of polymer processing, this structural recovery is of large importance for the final properties of the polymer composites after solidification. The reformation of the filler network takes place in the melt, so it is important to understand its origin and kinetics. For the final properties of conductive polymer composite, it is also important how the actual structure of the filler network is frozen-in during crystallization and vitrification.

It is the idea of this study to investigate the influence of shear and crystallization on the electrical and dielectric properties of CNT–polymer composites, with special focus on structural changes in the contact region between tubes. In the case of shear experiments the main interest is the kinetics of conductivity recovery after shear. Apart from scientific interest, the influence of mechanical stress or strain on the conductivity is of large practical interest for processing of CNT–polymer composites, since different volume elements can experience different thermal and mechanical prehistory during extrusion or melt injection. The extraordinary decrease in electrical conductivity with increasing shear rate was reported on nanotube-filled polypropylene [18]. However, in this study only steady shear flow was applied and no recovery experiments have been performed. In order to achieve conditions which are similar to melt processing, our experiments were performed in a slit die designed for in-line conductivity spectroscopy. This slit die was flanged to the outlet of a laboratory extruder.

Although it is well known that carbon nanotubes can act as specific nucleating agents in semi-crystalline polymers [19–22], studies on the influence of the crystalline phase on the structure of the CNT–polymer composite using conductivity spectroscopy are not yet reported in literature. In order to follow the changes of the frequency dependent conductivity (AC conductivity) and the dielectric permittivity during crystallization of the melt, in a second experiment the slit die was cooled below the crystallization temperature of polypropylene after the shear effects are relaxed. This can be considered as a model experiment for understanding the behavior of a CNT–polymer composite during injection molding. Similar non-isothermal crystallization experiments followed by AC conductivity measurements have been recently reported by some of us using poly(ethylene glycol) inside a test tube [23].

The conductivity recovery experiments are explained by reformation of a conductive filler network after breakdown of this structure and (possibly) orientation of dispersed nanotubes by shear flow. The reformation kinetics of the filler network is discussed in the framework of recovery of viscoelastic properties in filled elastomers, see e.g. Refs. [24,25], which was recently extended to the kinetics of modulus recovery in polyethylene with nanofillers, see Ref. [26] and references therein. The kinetics of forming new conductive contacts between CNT after breakdown of the network-like structure under shear can be interpreted as a cooperative reformation of a hierarchy of complex structures. This can be related to the ‘‘regulation in complex systems’’ (see e.g. Ref. [27]), known e.g. from autocatalytic reactions in chemistry or structure and reactivity of enzymes in biology. However, for conductive networks the structural kinetics has to be coupled to the percolation theory (see e.g. Refs. [16,23] and references therein) containing elements with different conductivities and/or permittivities.

The results of the crystallization experiments are also discussed in the framework of electrical percolation, where conductivity and permittivity of the matrix and the contact regions between nanotubes are changing during formation of a less conductive crystalline phase.

2. Experimental

2.1. Materials and composite preparation

The nanotubes used in this study were multiwalled carbon nanotubes (MWNTs) supplied as a PP masterbatch containing 20 wt% MWNT from Hyperion Catalysis International, Inc. (Cambridge, USA). The MWNT were produced by chemical vapour deposition (CVD) and have diameters of approximately 10 nm. According to the supplier, the length of the multiwalled carbon nanotubes is at least 10 μm after production with CVD, such that the aspect ratio is about 1000 [28]. In a previous processing step this masterbatch was diluted with polypropylene Moplen HF500N (Basell Polyolefins) using a ZSK-30 extruder (Coperion Werner & Pfleiderer) at 200–220 °C in order to get MWNT contents of 2, 3.5, and 5 wt%, which correspond to 1.03, 1.80, and 2.57 vol% assuming a MWNT density of 1.75 g/cm^3 [29]. Mixing was performed

at a rotational speed of 250 rpm and a throughput of 10 kg/h starting from granular premixtures. After the mixing, the extruded material was granulated.

Scanning electron microscopic (SEM) images of cryofractured surfaces prepared from granules of the PP masterbatch and the sample with 2 wt% MWNT are shown in Fig. 1. A XL30 ESEM-FEG (Philips) operating at high vacuum mode was used.

DC measurements of volume conductivity at room temperature were performed using a Keithley Electrometer 6517A on plates with a thickness of 0.35 mm. The plates were pressed at 220 °C, the granules were hold for 3 min in the press, and a pressure of 10 bar was applied for 1 min before the sample was cooled between two cold metal blocks. The results revealed that the sample containing 2 wt% MWNT (9.3×10^{-5} S/m) is close to the percolation threshold, whereas the MWNT in the other two samples (5.3×10^{-2} S/m for 3.5 wt% and 0.41 S/m for 5 wt%) are clearly above that threshold. Neat PP showed a conductivity of about 10^{-17} S/m.

2.2. In-line experiments

For the in-line experiments the premixed nanocomposite material was extruded using a single screw laboratory extruder (KE 19, Brabender OHG) into the measurement slit die until the melt channel was filled [30,31]. This slit die was equipped with dielectric sensors which are arranged in plate–plate geometry. The melt temperature was about 220 °C and the screw speed was 40 rpm. The throughput under these conditions is about 500 g/h. Taking the cross-section of the melt channel of 4×20 mm^2 into account and assuming a melt density of 800 kg/m^3 this results in a shear rate of approximately 2 s^{-1} at the channel walls.

In order to investigate the time dependent changes (in AC conductivity) under quiescent melt conditions the extruder was stopped for the measurements of the dielectric spectra. The melt temperature was tried to hold for 1200 s at about 220 °C. The initial melt temperature measured at the wall of the die was about 225 °C and was decreasing during this experiment to about 210 °C which is considered to be ''pseudo-isothermal''. All frequency spectra were recorded continuously from low to high frequencies needing about 30 s for a full frequency sweep. For more clarity only selected spectra are shown (see Figs. 5 and 10 below) where the time and the temperature at which the frequency sweeps were finished are assigned to the curves.

For studying the dielectric behavior upon cooling and crystallization the heating of the slit die was stopped and the melt was cooled down freely to room temperature until crystallization and delamination of the material from the wall occurred. During cooling dielectric spectra were recorded down to temperatures of about 100 °C. It could be ensured that the material was in contact with the sensor within the temperature range discussed in this paper.

2.3. Dielectric measurements

The measurement slit die equipped with dielectric sensors shown in Fig. 2 was recently developed to monitor the extrusion of conductive polymer composites [30,31]. The sensors (electrode diameter: 8 mm) were mounted face to face in the melt channel with a distance of 4 mm. The air capacitance was calculated by a finite element simulation of the electrical field for the actual sensor geometry, resulting in a value of 0.09 pF. An Agilent LCR bridge HP4284A was used to measure parallel capacitance C_p and $\tan\delta$ in a frequency range from 20 Hz to 1 MHz. The real parts of the complex permittivity ε' and conductivity σ' spectra are obtained from the air capacitance and the measured values of C_p and $\tan\delta$, respectively. The lower conductivity limit of the LCR bridge is about 10^{-7} S/m. Therefore, for neat PP no reliable values could be obtained by this setup.

In addition to the dielectric sensors the measurement slit die contains two pressure transducers for the determination of the mean and difference pressure, so that the die can be used as in-line rheometer. The design of the channel is based on a rheometric measuring die from Brabender (Germany). Two ultrasonic transducers (the data are not discussed in this paper) are placed between the pressure transducers.

3. Results and discussion

3.1. Conductivity and permittivity recovery after shear flow

The first conductivity spectra for polypropylene–carbon nanotube composites recorded during about 120 s after the

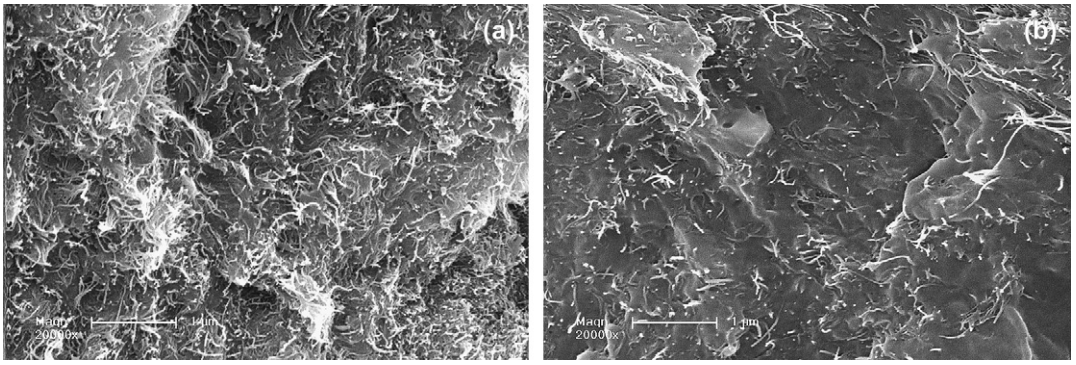

Fig. 1. SEM images of cryofractured surfaces prepared from granules of the PP masterbatch containing 20 wt% MWNT (a) and the sample with 2 wt% MWNT used for the conductivity spectroscopy (b).

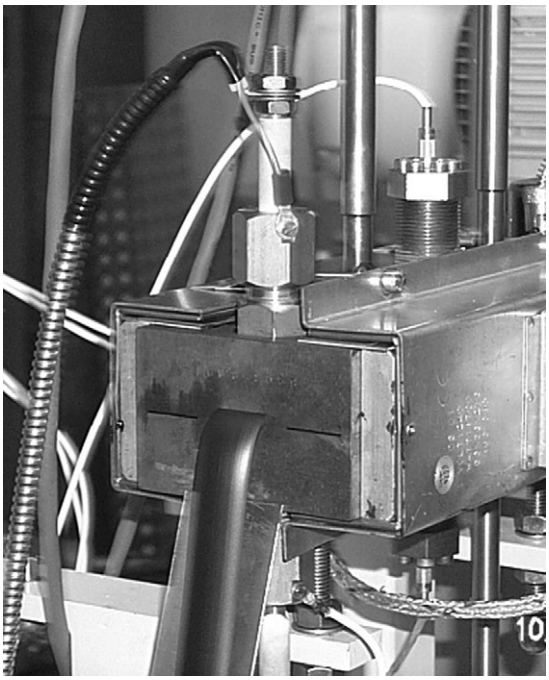

Fig. 2. Measurement slit die equipped with two dielectric sensors, two pressure transducers and two ultrasonic transducers.

extruder was stopped are shown in Fig. 3 for all three CNT concentrations. It is obvious from the conductivity spectra and shape of the curves (see e.g. Ref. [16]) that the sample containing 2 wt% MWNT is close to the percolation threshold, whereas the samples with 3.5 and 5 wt% are above that. Comparing these spectra with the volume conductivity data measured at room temperature on pressed plates (values named in Section 2.1) it is seen that the general trends are similar. However, the conductivity values measured in the melt at 220 °C immediately after stopping the extruder are lower as compared to the values obtained on solidified samples. It should be mentioned that the absolute difference depends strongly on both the prehistory of the solidified samples and the actual state of the melt.

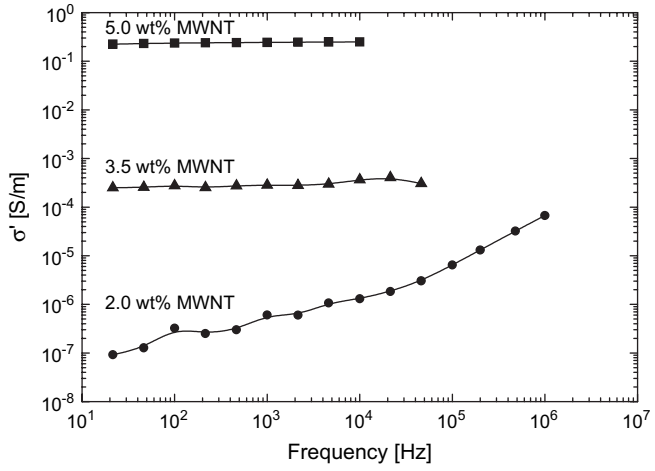

Fig. 3. Conductivity spectra for polypropylene–carbon nanotube composites with different MWNT contents recorded at about 120 s after the extruder was stopped. The temperature of the slit die was about 225 °C. The actual amount of MWNT is indicated in the figure.

Fig. 4 shows the time dependence of the conductivity measured at a frequency of 1 kHz for the polypropylene–carbon nanotube composites containing 2, 3.5, and 5 wt% MWNT, respectively, after the extruder was stopped. The initial melt temperature (measurement at the wall of the die) was about 225 °C and changed only slightly to about 210 °C during the observation time (1200 s). Therefore, the measurements in this interval were considered to be almost "pseudo-isothermal" since the decrease in the conductivity of the polymer matrix is negligible in this small temperature range.

It can be seen that the conductivity for the sample with 2 wt% MWNT increases tremendously with time, whereas the changes for the samples containing 3.5 and 5 wt% MWNT are not that significant.

The corresponding changes in the permittivity and conductivity spectra for the sample containing 2 wt% MWNT are represented in Fig. 5a and b versus frequency, whereas Fig. 6a and b shows the values at 10 kHz versus annealing time, respectively. The increase in the low frequency conductivity (the conductivity at $f = 1$ kHz is taken for the DC conductivity) by about four orders of magnitude as seen in Fig. 4c and of the permittivity at 1 kHz by a factor of 100 (see Fig. 5a) can be explained by reformation of the conductive MWNT

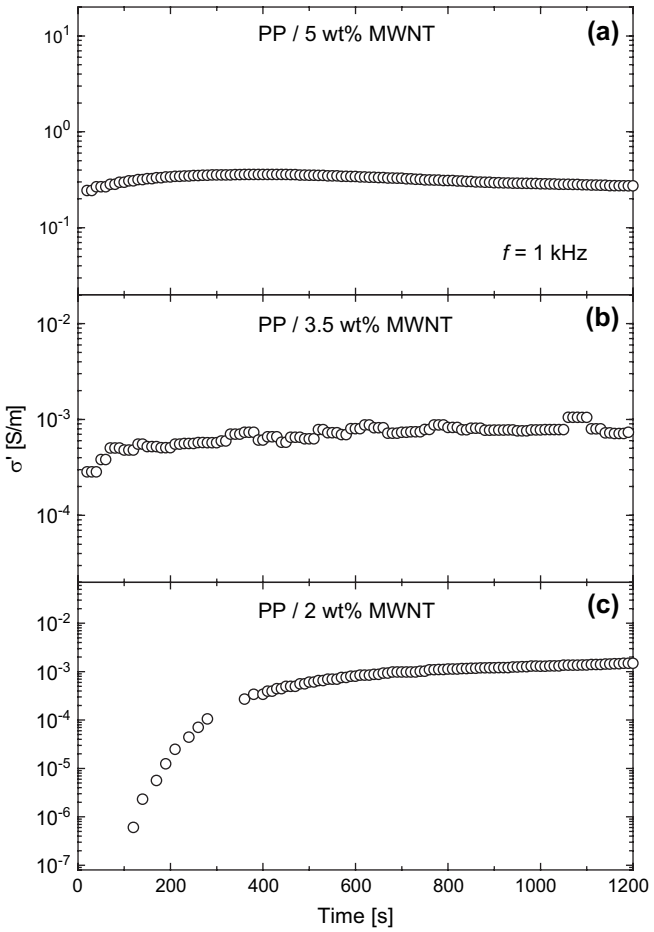

Fig. 4. Time dependence of the conductivity measured at a frequency of 1 kHz for three polypropylene–carbon nanotube composites containing 2, 3.5, and 5 wt% MWNT, respectively, recorded after the extruder was stopped.

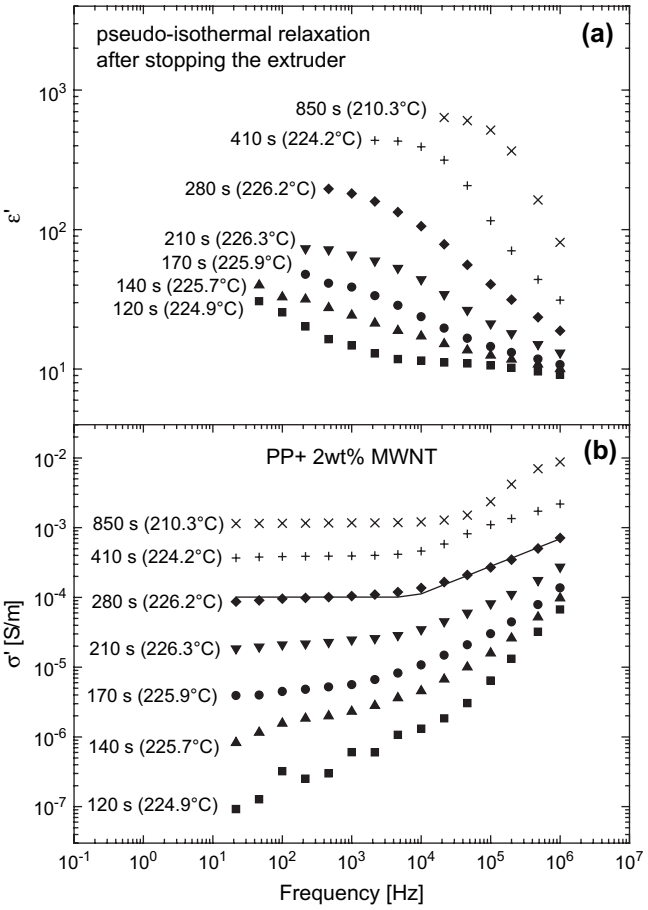

Fig. 5. Frequency dependence of permittivity (a) and conductivity (b) for the composite with 2 wt% MWNT during pseudo-isothermal annealing after stopping the extruder (temperature range from 226.3 °C to 210.3 °C, only selected spectra are shown). As an example, the fitted curve for σ' (as described in the text) is shown for $t = 280$ s.

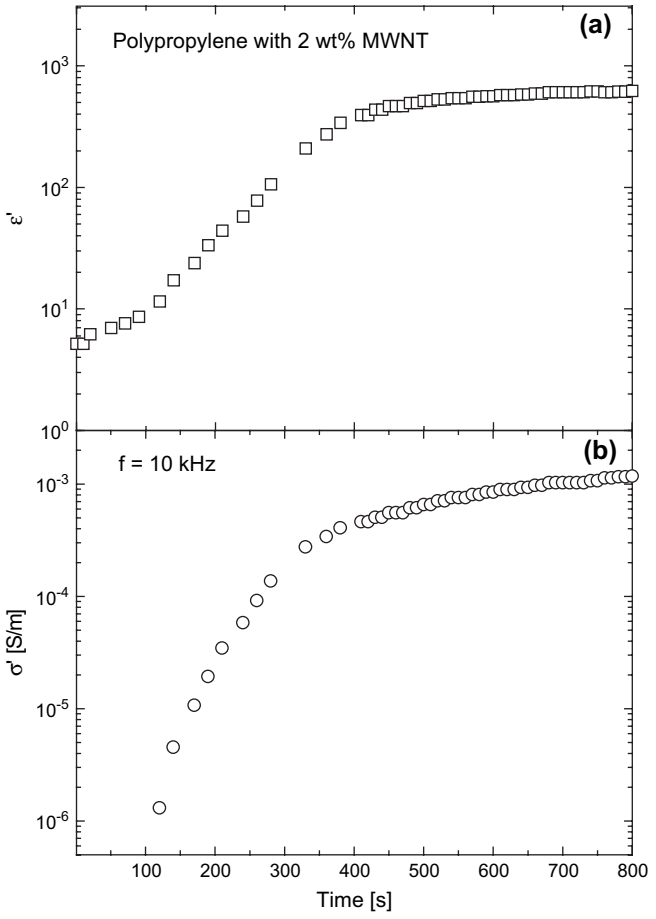

Fig. 6. Permittivity (a) and conductivity (b) at 10 kHz for the composite with 2 wt% MWNT versus annealing time after stopping the extruder (temperature range from 226.3 °C to 210.3 °C).

structure. Possibly, the nanotubes rearrange to form a hierarchy of conductive structures on a mesoscopic scale (clusters of different shapes and sizes). At the same time, the polymer chains in the contact region between the tubes which have been disrupted by the shear field rearrange on a local length scale and form nanoscopic bridges. In addition to the local reformation in the contact regions, the reorientation of the tubes that oriented before in the shear flow has to be taken into account. The lower significance of shear induced breakdown and reformation of the conductive network for samples with higher MWNT content (see Fig. 4a and b) can be explained by the higher amount of remaining percolation passes after shear and/or elongational deformation.

In order to get an idea on the mechanism of reformation of the conductive percolation network in the quiescent melt, in Fig. 7 the conductivity at 10 kHz was plotted in a double-logarithmic plot. Although it is somewhat difficult to find the exact time where the melt starts to rest (after stopping the extruder, the flow does not stop immediately and the time interval for recording the spectra results in an additional time error in the range up to 100 s), the curve tends to level off for long rest (annealing) times. Such a behaviour can be described by a combination of percolation theory and network recovery as it was discussed in Ref. [26] for carbon black networks. In order to study this in more detail, better defined offline experiments with a laboratory rheometer equipped with a dielectric plate geometry are in progress. The first results confirm the findings for the slit die geometry.

The conductivity spectra as shown in Fig. 5 were analyzed quantitatively in the frame of percolation theory. Therefore some of the basics are summarized in the following paragraph. It has been established, both theoretically and experimentally, that near the critical concentration φ_c the DC conductivity and the static permittivity show power-law behavior [36–42]:

$$\sigma_{DC} \equiv \sigma'(\varphi, f = 0) \propto (\varphi_c - \varphi)^{-s}, \quad \varphi < \varphi_c \tag{1}$$

$$\sigma_{DC} \equiv \sigma'(\varphi, f = 0) \propto (\varphi - \varphi_c)^{t}, \quad \varphi > \varphi_c \tag{2}$$

$$\varepsilon_s \equiv \varepsilon'(\varphi, f = 0) \propto |\varphi - \varphi_c|^{-s'}, \quad \varphi < \varphi_c,\ \varphi > \varphi_c \tag{3}$$

where f is the measurement frequency. The critical exponents s and t are assumed to be universal, i.e. they depend only on the dimension of the percolation system and not on the details of cluster geometry [32,36–42]. The real part of the conductivity

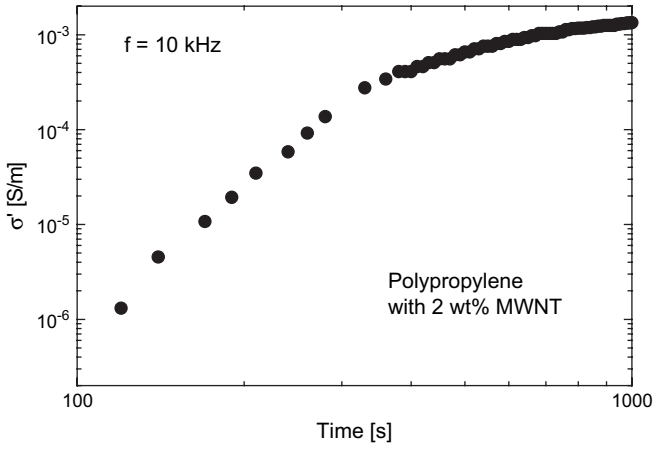

Fig. 7. Double-logarithmic representation of conductivity at 10 kHz for the composite with 2 wt% MWNT versus recovery time (data from Fig. 6).

near the percolation threshold was also predicted to follow a power-law [39–41]:

$$\sigma'(f) \propto f^n \tag{4}$$

The currently accepted values for the critical exponent n [32–35] in 2D ($d=2$) and 3D ($d=3$) are 0.5 and ≈ 0.72 for the equivalent circuit model, and ≈ 0.34 and ≈ 0.6 for anomalous charge carrier diffusion, respectively. The equivalent circuit model [36–44] assumes a random mixture of capacitors and resistors forming the percolation clusters. In the charge carrier diffusion model [45–53], it is assumed that for frequencies $f < f_c$ the charge carriers can explore different clusters within one period, i.e. the diffusion is normal. For frequencies above f_c the charge carriers visit only parts of the percolation cluster within one period and anomalous diffusion at the fractal percolation clusters takes place. This critical frequency f_c also follows a power law:

$$f_c \propto \frac{1}{\tau_\xi} \propto |\varphi - \varphi_c|^{\nu d_w} \tag{5}$$

where ν is the critical exponent related to the cluster size [33,34] and d_w is the effective fractal dimension of the random walk. The correlation time τ_ξ is the time needed by the charge carriers to transverse (“explore”) a percolation cluster of the correlation length ξ.

From the experimental curves in Fig. 5 the DC conductivity σ_{DC}, the cross-over frequency f_c, and the exponent n of the power-law function at high frequencies have been estimated. To obtain these three parameters a non-linear curve fitting procedure was applied to fit the σ' versus f data. The following function was used:

$$\sigma'(f) = \begin{cases} \sigma_{DC} & |f < f_c \\ \sigma_{DC}(f/f_c)^n & |f \geq f_c \end{cases}$$

The fitting was done in OriginLab Origin®, using a *Y*-script of the following form:

```
y=SDC;
if(x>=FC) y=SDC*(x/FC)^N;
```

In this script, SDC, FC, and N are the parameters corresponding to σ_{DC}, f_c and n. The dependent variable is y (conductivity), and the independent variable is x (frequency).

As an example, the fitted curve for σ' is shown in Fig. 4 for $t = 280$ s. The parameters resulting from this fit are $\sigma_{DC} =$ 1.0E-4 ± 5.2E-6 S/m, $f_c = 7632 \pm 1485$ Hz and $n = 0.395 \pm 0.013$. Due to the limited frequency range and the time shift between the frequency points of one spectra the fit was only possible between $t = 170$ s and $t = 380$ s. Between $t = 280$ s and $t = 360$ s the spectra could not be properly recorded due to balancing problems of the LCR bridge so that data analysis for this time interval was not possible. At times above 400 s after stopping the extruder an additional relaxation process, most probably originating from polarization of the microcapacitors formed by the bound rubber, is dominating the conductivity spectra and prevent the analysis in the frame of a simple percolation picture.

The results of this analysis versus annealing time are summarized in Fig. 8. It is seen that σ_{DC} is increasing, f_c is slightly increasing, and n is decreasing with annealing time after shearing was stopped.

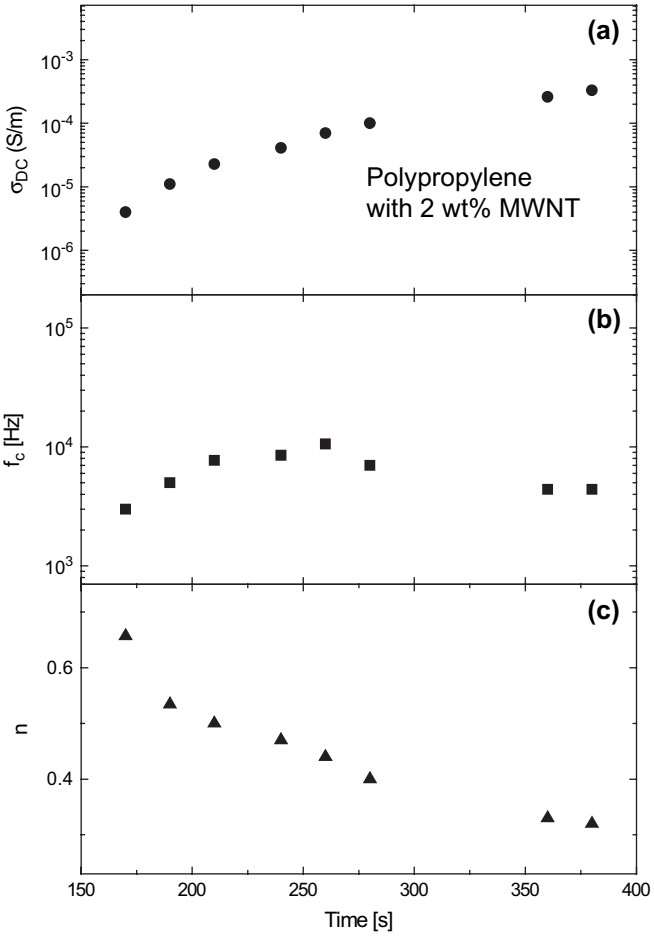

Fig. 8. Changes in the DC conductivity σ_{DC} (a), the cross-over frequency f_c (b), and the power n of the frequency dependence of the AC conductivity (c) for the composite with 2 wt% MWNT during annealing. The fits are obtained from the conductivity spectra as shown in Fig. 5.

The features for all three quantities can be described in a percolation picture by a gradual change of the difference between the effective concentration of electrical active filler particles (or bonds) and the (idealized) percolation threshold, assuming that all conductive sites or bonds contribute. In this picture the reduction of the conductivity by shear can be explained by a reduction of conductive links (which is identical to a reduction of the effective amount of conductive filler particles) by rupture of the CNT contacts due to mechanical deformation. Therefore, the time development of σ_{DC}, f_c, and n in Fig. 8 is a representation of the partial recovery of the idealized percolation structure for the given concentration. The simultaneous increase in σ_{DC} and f_c is an indication that the system is above the percolation threshold (Eqs. (2) and (5)). The decrease in n is related to an increasing distance to the threshold. Since Eqs. (4) and (5) hold only close to the percolation threshold a conclusion on the type of percolation is difficult. The variation from about 0.7 to about 0.3 is in the range of the predicted critical exponents for 2D or 3D.

Up to here, our discussion was focused on the conductivity data. However, the dielectric permittivity ε' and its static (low frequency) value ε_s show a similar recovery during the rest time. The assumption of a combined nanotube–polymer–nanotube network (highly conductive nanotubes are separated in their local contact regions by polymer chains) as discussed in one of our previous papers (see Ref. [17]) is supported by the high permittivity values (about 10^3, see Figs. 5a and 6a) for the almost recovered percolation network above the percolation threshold.

Since the $\varepsilon'(f \to 0)$ becomes very small well above the threshold (see Eq. (3)) these high permittivity values can only be explained by assuming small capacitors at the tube contacts.

In this picture, the shear stress is expected to destroy the CNT–polymer–CNT contact regions leading to a tremendous increase in the contact resistance and a decrease in the contact capacitance C even for slight increase in the local tube distance d ($C \sim 1/d$).

In this context it has to be taken into consideration that the carbon nanotubes can orient along the flow direction. Recently, Hobby et al. [54] showed using polarized light-scattering experiments on a weakly elastic melt that the tubes orient along the direction of flow already at low shear stresses, with a transition to vortices alignment above a critical shear stress. For highly elastic polymer solutions the tubes are found to orient with shear field at high shear fields. Although these investigations were performed at very dilute systems (mass fraction of MWNT of 1.7×10^{-3}) using MWNT with an extremely large aspect ratio and large persistence length (1–10 μm), this effect cannot be excluded for our systems (smaller tube length, larger curvature and higher melt viscosity). This orientation of the CNT is not included in actually used percolation models assuming isotropic distribution and orientation of the fillers. For an electrical field perpendicular to the flow direction, the orientation of the tubes would act like an effective reduction of the aspect ratio. This would shift the percolation threshold for measurements perpendicular to the main axis of the tubes to higher concentration.

3.2. Cooling and crystallization

After investigation of the effect of annealing, the heating of the extruder die was stopped and the cooling and crystallization behavior were studied. Fig. 9 shows the permittivity and conductivity at 1 kHz for the composite with 2 wt% MWNT during cooling from 180 °C to 120 °C. The values at 1 kHz can be taken to be representative for the DC conductivity σ_{DC} and static permittivity ε'_s. The drastic decrease in permittivity and conductivity at about 140 °C indicates the crystallization of the sample.

The corresponding spectra for $\sigma'(\omega)$ and $\varepsilon'(\omega)$ are depicted in Fig. 10. The conductivity spectra show the typical crossover behavior from a DC conductivity plateau at low frequencies to a power-law dependence of σ' (e.g. charge carrier diffusion in a percolation structure).

As shown in Fig. 9b, the DC conductivity decreases by more than one order of magnitude in the temperature interval of crystallization. This can be explained by the reduction of the amount of amorphous phase (where ion conductivity is the dominating conduction mechanism) on expense of the almost non-conducting crystalline phase. Usually the charge carriers are trapped in or at the surface of the crystalline lamellae. Furthermore, the conducting passes become restricted by the growth of crystalline lamellae and spherulites. This results

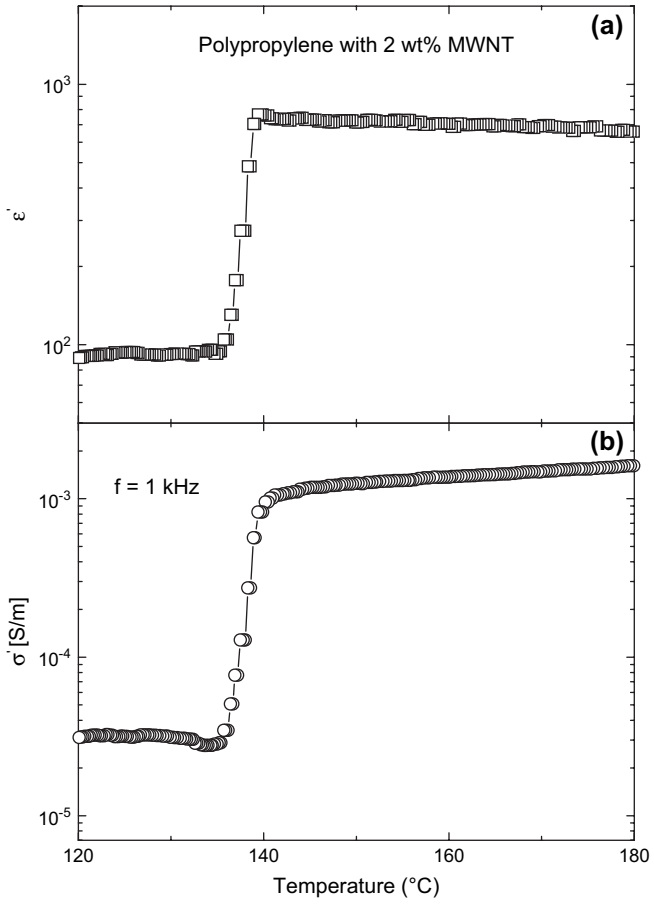

Fig. 9. Permittivity (a) and conductivity (b) at 1 kHz for the composite with 2 wt% MWNT during cooling from 180 °C to 120 °C.

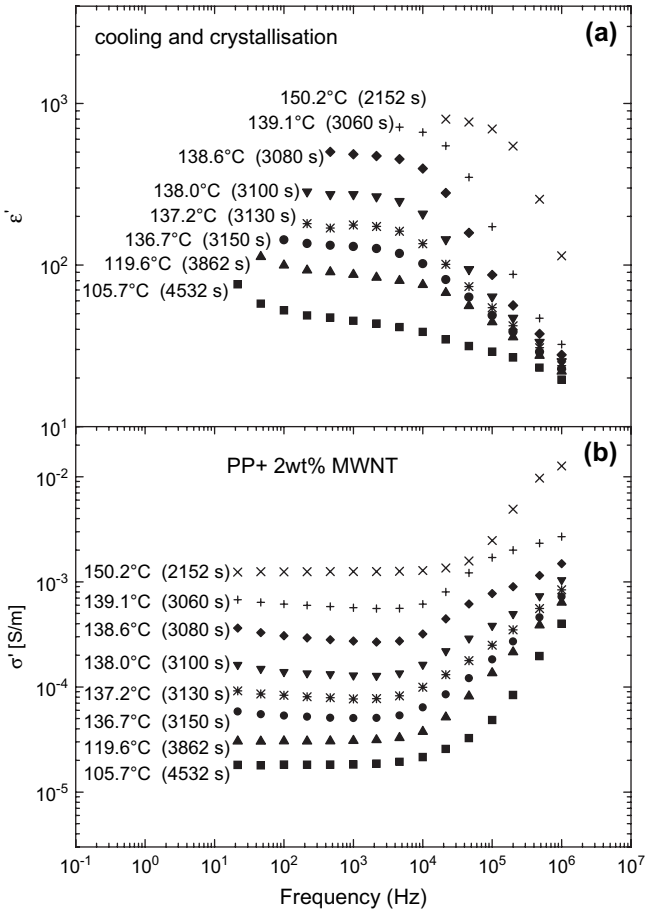

Fig. 10. Frequency dependence of permittivity (a) and conductivity (b) for the composite with 2 wt% MWNT recorded during cooling and crystallization. The actual temperatures at the end of each measurement run are indicated in the figure (only selected spectra are shown).

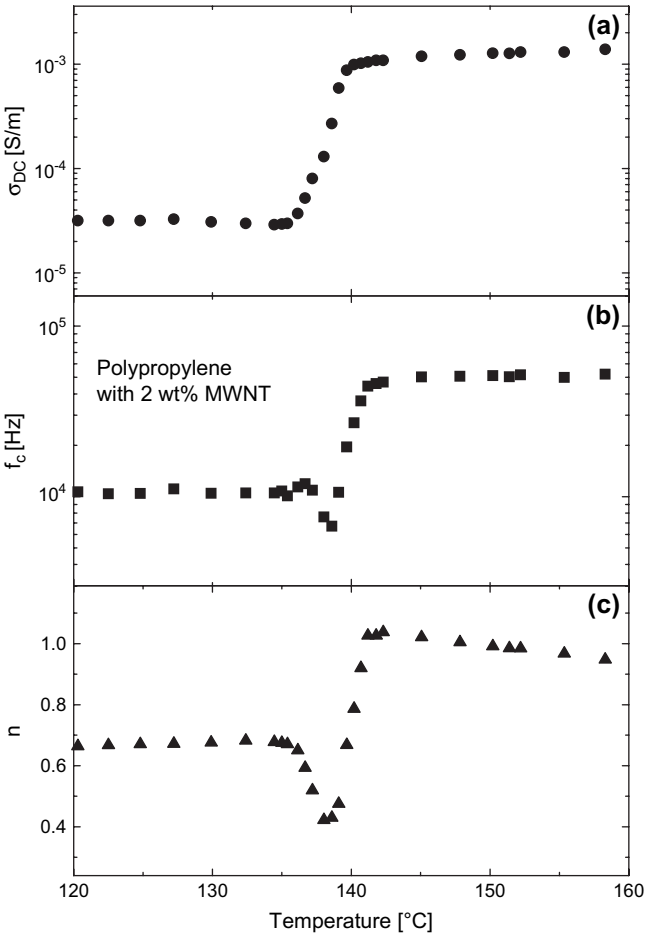

Fig. 11. Changes in the DC conductivity σ_{DC} (a), the cross-over frequency f_c (b), and the power n of the frequency dependence of the AC conductivity (c) for the composite with 2 wt% MWNT during cooling from 180 °C to 120 °C. The fits are obtained from the conductivity spectra as shown in Fig. 10.

in a fractal structure for the remaining amorphous phase [23] which is possibly bridged by the nanotubes.

Since the nanotubes act as nuclei for crystallization, an insulating transcrystalline layer around the CNT may form. However, from measurements of conductivity alone (integrating over a large volume) it cannot be differentiated between these possible mechanisms.

The decrease in the low frequency permittivity (see Fig. 10a) during crystallization can also be related to the decreased conductivity of the amorphous phase in an indirect manner (e.g. by decrease in the conductivity in the contact regions). A more detailed interpretation of the permittivity spectra taking surface polarization and relaxation processes into account is possible (see Ref. [23]), but would be rather arbitrary for the accuracy of the data measured in a technical setup.

In order to achieve a more quantitative analysis of the conductivity spectra recorded in the temperature interval of crystallization, in Fig. 11 the values for σ_{DC}, f_c, and n as extracted from Fig. 10 are shown. While σ_{DC} is decreasing continuously with decreasing temperature, n and possibly f_c pass through a minimum.

Such behavior is typical for a system passing a critical point (see Eqs. (1)–(5). At the percolation composition p_c, the cross-over frequency f_c is expected to approach zero (the charge carriers have to explore the ''infinite cluster'' which needs ''infinite time''), whereas n should approach its critical value at p_c corresponding to the dimension of the lattice. Due to the time interval needed for one frequency sweep (of about 30 s) and the fast crystallization kinetics, the critical slowing down in f_c cannot be resolved in detail. However, the minimum in f_c at about 138 °C seems to indicate the percolation threshold for the effective concentration of fillers (or contacts). Assuming now that the exponent of the frequency dependence of σ' (see Eq. (4)) is related to a situation close to the threshold, the exponent of about 0.4 is in the order of the accepted values for 3D anomalous charge carrier diffusion ($n \approx 0.34$–0.6 for 2D and 3D). The values for the equivalent circuit model vary between 0.5 for 2D and 0.72 for 3D. Although the estimation of f_c and n is somewhat arbitrary, the following conclusions can be drawn in the frame of the percolation theory: (i) the system changes during crystallization from a situation above the percolation threshold to a conductivity below p_c and (ii) the time dependent ''effective percolation concentration'' is due to morphological changes in the semi-crystalline structure of the composite, since the MWNT concentration does not change in the process of

crystallization. The second conclusion supports the assumption that the electrical percolation network has to be considered as a combination of nanotubes and polymer in the contact regions between nanotubes. The crystallization of the polymer matrix alone, i.e. without changes in the conductivity of ''polymeric synapses'' between the tubes, would only decrease the total conductivity, but cannot explain a ''passing through'' of the percolation threshold for a constant CNT content. In other words, the change of state of ''polymeric synapses'' acts like a change of the ''effective content'' of conducting sites, by decreasing the conductive bonds between tubes and/or clusters. Following the discussion given above for the breaking of ''conductive bonds'' by shear, one can assume here a reduction of ''conductive bonds'' by structural changes (crystallization) of the chains in the contact region.

4. Summary and conclusions

In this paper, frequency dependent conductivity measurements were presented on multiwalled carbon nanotube–polypropylene composites in the molten state. Both annealing of the MWNT–PP samples in the melt after shear stress and crystallization and solidification behaviour were studied. A slit die with dielectric sensors designed for in-line monitoring of polymer processing was applied to monitor carbon nanotube-filled polypropylene during extrusion, during annealing without shear and during crystallization. The main results can be summarized as follows:

(1) The percolation threshold of MWNT in melt mixed polypropylene composites was found to depend dramatically on the prehistory. For a sample containing 2 wt% MWNT, the DC conductivity in the sheared melt at 220 °C is less than 10^{-7} S/m, whereas the value in the annealed melt (20 min after stopping the extruder) increased to about 1.4×10^{-3} S/m. The DC conductivity of a plate measured at room temperature and prepared by pressing the composite granules at 220 °C is 9.3×10^{-5} S/m. This effect is less pronounced for samples with 3.5 and 5 wt% MWNT which are clearly above the percolation threshold. The difference in conductivity values can be explained by a strong dependence of the ''effective number of conducting bonds'' on the arrangement of the nanotubes and clusters in the matrix as well as on the arrangement of the polymer chains in the gaps between the tubes. All these effects depend strongly on the thermo-mechanical prehistory of the sample.
(2) The DC conductivity and the static permittivity were found to increase with annealing (rest time after shear was stopped) of the melt for the sample with 2 wt% MWNT. This behavior is consistently expressed in the AC conductivity and permittivity spectra, which were analyzed in the frame of percolation theory. The annealing behavior of CNT–polymer composites was found to be similar to the behavior of carbon black polymer composites and is addressed to breaking and reformation of (micro-) capacitors and resistors formed at the nanotube–nanotube contacts.
(3) The reformation kinetics cannot be explained by translational or rotational diffusion of nanotubes alone. The power-law-like behavior for long rest times is addressed to a cooperative structure formation in complex systems (e.g. cluster–cluster aggregation). Since the dimension of the nanotube spans from several nanometer (diameter) to several micrometer (length), the kinetics is expected to couple to relaxation processes at different time scales.
(4) The crystallization has been found to have a significant effect on the conductivity and permittivity of CNT–polymer composites. At CNT contents near p_c, the decrease in conductivity due to crystallization is more pronounced than for samples with a CNT content well above p_c. The influence of crystallization on the dielectric and conductivity spectra cannot only be explained by changes of conductivity and permittivity of the matrix. For explanation of the changes in the cross-over frequency and the exponent of the frequency dependence a percolation picture has to be used, taking into account the changes of conductivity and capacitance in the contact region due to crystallization.

The results presented here clearly show that dielectric conductivity spectroscopy is a viable method for the characterization of the interplay between processing condition, structure of the conducting network, and dielectric properties of melt processed CNT–polymer composites. Furthermore, it was shown that the in-line application of these methods yields a useful tool for monitoring the electrical and dielectric properties of CNT–polymer composites during processing.

Experiments on CNT–polymer composites by using a combination of rheometer (plate–plate geometry) with dielectric spectroscopy (the plates of the rheometer act as the capacitor plates) are in progress. From these experiments it is expected to get a deeper and more quantitative understanding of the coupling between shear induced network rearrangements and dielectric properties.

Acknowledgments

This project is funded by the Bundesministerium für Wirtschaft und Arbeit via the Arbeitsgemeinschaft industrieller Forschungsgesellschaften (AiF Project No. 122Z and No. 14454N). Additional financial support is given by the Forschungsgesellschaft Kunststoffe e.V. We thank Hyperion Catalysis International, Cambridge, USA for providing the polypropylene masterbatch. Bernd Kretzschmar (IPF) is thanked for preparing the nanocomposites using masterbatch dilution. We would like to thank Professor Gert Heinrich (IPF) and Martin Engel (DKI) for the illuminating discussion, and Sven Pegel (IPF) and Quame Quarteng (MLU Halle) for their help in the experiments.

References

[1] Thostenson ET, Li C, Chou TW. Compos Sci Technol 2005;65:491–516.
[2] Breuer O, Sundararaj U. Polym Compos 2004;25(6):630–45.

[3] Coleman JN, Khan U, Gun'ko YK. Adv Mater 2006;18(6):689–706.
[4] Sandler JKW, Kirk JE, Kinloch IA, Shaffer MSP, Windle AH. Polymer 2003;44(19):5893–9.
[5] Jiang X, Bin Y, Matsuo M. Polymer 2005;46:7418–24.
[6] Andrews R, Jacques D, Minot M, Rantell T. Macromol Mater Eng 2002; 287:395–403.
[7] Coleman JN, Cadek M, Blake R, Nicolosi V, Ryan KP, Belton C, et al. Adv Funct Mater 2004;14:791–8.
[8] Satapathy BK, Weidisch R, Pötschke P, Janke A. Macromol Rapid Commun 2005;26(15):1246–52.
[9] Gorga RE, Cohen RE. J Polym Sci Part B Polym Phys 2004;42(14): 2690–702.
[10] Kashiwagi T, Grulke E, Hilding J, Groth K, Harris R, Butler K, et al. Polymer 2004;45:4227–39.
[11] Yang Z, Dong B, Huang Y, Liu L, Yan FY, Li HL. Mater Chem Phys 2005;94:109–13.
[12] Zilli D, Chiliotte C, Escobar MM, Bekeris V, Rubiolo GR, Cukierman AL, et al. Polymer 2005;46:6090–5.
[13] Haggenmueller R, Gommans HH, Rinzler AG, Fischer JE, Winey KI. Aligned single-walled carbon nanotubes in composites by melt processing methods. Chem Phys Lett 2000;330:219–25.
[14] Tang W, Santare MH, Advani SG. Carbon 2003;41(14):2779–85.
[15] Pötschke P, Bhattacharyya AR, Janke A, Pegel P, Leonhardt A, Täschner C, et al. Fullerenes Nanotubes Carbon Nanostruct 2005;13(1):211–24.
[16] Pötschke P, Dudkin SM, Alig I. Polymer 2003;44:5023–30.
[17] Pötschke P, Abdel-Goad M, Alig I, Dudkin SM, Lellinger D. Polymer 2004;45:8863–70.
[18] Kharchenko SB, Douglas JF, Obrzut J, Grulke E, Migler KB. Nat Mater 2004;3:564–8.
[19] Grady BP, Pompeo F, Shambaugh RL, Resasco DE. J Phys Chem B 2002;106:5852–8.
[20] Valentini L, Bigotti J, Kenny JM, Cantucci S. J Appl Polym Sci 2003;87: 708–13.
[21] Bhattacharyya AR, Sreekumar TV, Liu T, Kumar S, Ericson LM, Hauge RH, et al. Polymer 2003;44:2373–7.
[22] Assouline E, Lustiger A, Barber AH, Cooper CA, Klein E, Wachtel E, et al. J Polym Sci Part B Polym Phys 2003;41:520–7.
[23] Alig I, Dudkin SM, Jenninger W, Marzantowicz M. Polymer 2006;47: 1722–31.
[24] Heinrich G, Klüppel M. Adv Polym Sci 2002;160:1–44.
[25] Klüppel M. Adv Polym Sci 2003;164:1–86.
[26] Heinrich G, Costa FR, Abdel-Goad M, Wagenknecht U, Lauke B, Härtel V, et al. Kautsch Gummi Kunstst 2005;58:163–6.
[27] Nicolis G, Prigonine I. Exploring complexity. New York: H. Freeman and Company; 1989.
[28] <http://www.fibrils.com/technology2.htm/>; 2006 [accessed 06.10.06].
[29] Shaffer MSP, Windle AH. Adv Mater 1999;11:937–41.
[30] Alig I, Fischer D, Lellinger D. Macromol Symp 2006;230:51–8.
[31] Steinhoff B, Lellinger D, Alig I, Pötschke P. PPS-21, Conference proceedings (ISBN 3-86010-784-4); 19–23 June 2005. SL 15-9.
[32] Clerc JP, Giraud G, Laugier JM, Luck JM. Adv Phys 1990;39(3): 191–309.
[33] Bunde A, Havlin S. Fractals and disordered systems. Berlin-Heidelberg/ New York: Springer; 1996.
[34] Stauffer D, Aharony A. Introduction to percolation theory. London: Taylor & Francis Ltd; 1994.
[35] Sahimi M. Applications of percolation theory. London: Taylor & Francis Ltd; 1994.
[36] Kirkpatrick S. Rev Mod Phys 1973;45:574–88.
[37] De Gennes PG. J Phys Lett (Paris) 1976;37:L1.
[38] Efros AL, Shklovskii BI. Phys Status Solidi B 1976;76:475–85.
[39] Straley JP. J Phys C Solid State Phys 1976;9:783–95.
[40] Bergman DJ, Imry Y. Phys Rev Lett 1977;39(19):1222–5.
[41] Webman I, Jortner J, Cohen MH. Phys Rev B 1977;16(6):2593–6.
[42] Stephen MJ. Phys Rev B 1978;17(11):4444–53.
[43] Stroud D, Bergman DJ. Phys Rev B 1982;25(3):2061–4.
[44] Wilkinson D, Langer JS, Sen PN. Phys Rev B 1983;28(2):1081–7.
[45] Scher H, Lax M. Phys Rev B 1973;7(10):4491–519.
[46] De Gennes PG. Recherche 1976;7:919.
[47] Stauffer D. Phys Rep 1979;54(1):1–74.
[48] Straley JP. J Phys C Solid State Phys 1980;13:2991–3002.
[49] Gefen Y, Aharony A, Mandelbrot BB, Kirkpatrick S. Phys Rev Lett 1981;47(25):1771–4.
[50] Gefen Y, Aharony A, Alexander S. Phys Rev Lett 1983;50(1):77–80.
[51] Weiss GH, Rubin RJ. Adv Chem Phys 1983;52:363–505.
[52] Laibowitz RB, Gefen Y. Phys Rev Lett 1984;53(4):380–3.
[53] Hong DC, Stanley HE, Coniglio A, Bunde A. Phys Rev B 1986;33(7): 4564–73.
[54] Hobby EK, Wang H, Kim H, Lin-Gibson S, Grulke EA. Phys Fluids 2003;15(5):1196–202.